Research Article

A Comparative Study of Thermal Behavior and Kinetics of the Rice Husk, Low-Density Polyethylene (LDPE) and Polyethylene Terephthalate (PET) for Pyrolysis

Divya Bisen[a], Ashish Pratap Singh chouhan[1a*], Raja Mohan Sakthivel[b]

[a] Department of physics, School of chemical engineering and physical science, Lovely professional University phagwara P. O. Box: 144401, India.
[b] Department of Mechanical Engineering, Govt. College of Technology, Coimbatore, P. O. Box: 641013, India.

P A P E R   I N F O

A B S T R A C T

Recently, waste materials have garnered attention for their potential in providing clean and affordable energy through thermochemical conversion techniques. They play a significant role in transforming waste into eco-friendly energy, but the proper selection of materials is crucial for successful thermochemical conversion. The primary objective of this study is to assess combustion efficiency based on activation energy, utilizing TGA and DTG analysis. Rice husk (RH), low-density polyethylene (LDPE), and polyethylene terephthalate (PET) waste materials were chosen for investigation. Experiments were conducted at temperatures ranging from 25 °C to 600 °C, with varying heating rates of 10, 20, 30, and 40 °C min^{-1}. The apparent activation energy of the feedstocks was determined using five different iso-conversional model-free approaches, namely Kissinger Akahira Sunose (KAS), Friedman, Flynn Wall Ozawa (FWO), Starink, and Tang methods. The apparent activation energy for rice husk, LDPE, and PET fell within the range of 113-123 kJ mol^{-1}, 101-101 kJ mol^{-1} and 105-117 kJmol^{-1}, respectively This research also contributes to establishing Comprehensive Pyrolysis Index (CPI) values to identify suitable sources for pyrolysis and gasification. According to CPI results, temperatures between 500 to 600 °C are optimal for pyrolysis, and an increase in heating rate enhances the output of pyrolysis products. A higher CPI index is favorable for achieving both a high calorific value and increased hydrocarbon contents.

https://doi.org/10.30501/jree.2024.416390.1688

1. INTRODUCTION[1]

India's energy prices have recently increased due to rising demand from industries, including domestic, commercial, and agricultural sectors. The continuous depletion of natural resources exacerbates this increase. Utilizing the plentiful supply of natural waste materials, such as plastic trash, rice leftovers, and municipal solid waste, offers a potential solution. In addition to addressing the increase in energy prices, this strategy aligns with sustainable standards and demonstrates a proactive approach to utilizing waste for a cleaner and more effective energy production system. Rice husk, a byproduct of India's significant rice production, has high energy content and can be effectively converted through pyrolysis into usable energy forms (Zhang et al., 2010).Research and development on biomass conversion technology must be accelerated to improve the effectiveness of using biomass as an alternative energy source in India (NPTEL, 2016). One key area of focus for India is the utilization of rice husk as a feedstock for energy production. Thermochemical conversion techniques, including pyrolysis, combustion, and gasification, highly depend on temperature and heating rate, directly affecting the output products. According to the literature survey, a temperature range of 500-600°C is suitable for pyrolysis with a rapid heating rate. However, low heating rates can reduce bio-oil and increase pyro gases and char contents, influenced by the degradation of cellulose, hemicellulose, and lignin contents in rice husk (Haiping Yang et al., 2007). For biomass gasification, a suitable temperature range is 600°C to 1100°C. This range breaks down hydrocarbons into producer gas, including water and tars, along with combustible gases like carbon monoxide (CO), hydrogen (H_2), methane (CH_4), and carbon dioxide (CO_2). The direct use of producer gas in industrial applications, such as gas turbines, internal combustion engines (ICE), and greenhouse heating in agricultural output, is hindered by tar and other hydrocarbon compounds Temperature range plays a significant role in the production of bio-oil in the pyrolysis process and producer gas in the gasification process. Temperature range plays a significant role in the production of bio-oil in the pyrolysis process and producer gas in the gasification process. Tar content can be removed by proper sample and temperature selection and heating rate (Rahman, 2022; Rahman et al., 2020). This study highlights wastes such as rice husk, LDPE, and PET for the estimation of kinetic parameters using TGA and DTG analyzers. Activation energy is determined using different differential and integral-based model-free methods. Activation energy and heating value are crucial parameters for estimating the best solid fuel for energy production through thermochemical conversion methods, such as pyrolysis, gasification, and combustion. The novelty in this work lies in studying the differential and integral methods for rice husk and low-density polyethylene (LDPE) and polyethylene terephthalate (PET) for pyrolysis. Further analysis using the Comprehensive Pyrolysis Index (CPI) assesses the suitability of solid waste for additional applications.

Importance of Isothermal and non-isothermal Kinetics

The degradation of conversion as a function of temperature and time is expressed by isothermal kinetic equations, which are based on Arrhenius parameters. The link between conversion and temperature and time is captured by isothermal conversion methods, often known as differential methods. Conversely, non-isothermal techniques, also known as integral techniques, only characterize conversion in the non-isothermal kinetic equation as a function of time (Vyazovkin and Charles, 1988).

The isothermal equation is given as:

$$d\alpha = \left(\frac{\partial \alpha}{\partial t}\right)_T dt + \left(\frac{\partial \alpha}{\partial T}\right)_t dT \qquad [1]$$

The non-isothermal equation is given as:

$$\frac{d\alpha}{dt} = \left(\frac{\partial \alpha}{\partial t}\right)_T + \beta \left(\frac{\partial \alpha}{\partial T}\right)_t [2]$$

2. EXPERIMENTAL

2.1 Material and Methods

In this research work, the rice husk (RH) was collected from agricultural fields at Barghat (MP), India. Other feedstock such as low-density polyethylene (LDPE) and polyethylene terephthalate (PET) were collected from different streets of Barghat (MP) India. The samples were first washed with

*Corresponding Author's Email: ashish.chouhan@gmail.com

 tap water and then sun-dried for 5 days to remove residual moisture. Next, it was oven-dried at 110 $^{\circ}$C temperature and the samples were taken for further testing and analysis.

3. METHOD

3.1. Methodology

The RH, PET, and LDPE samples underwent proximate and ultimate analysis. Proximate analysis, which included determining water content (WC), volatile matter (VM), fixed carbon (FC), and ash content (AC), was conducted in the muffle furnace. The calculation of fixed carbon (FC) was based on the difference. The elemental composition of all three blended samples was determined using an elemental analyzer to analyze carbon, hydrogen, nitrogen, and sulfur. The analysis was performed according to ASTM standards with a CHNS analyzer (Elementar Vario EL III). The oxygen content was calculated by the difference. The higher heating value (HHV) of a mixture of rice husk and low-density polyethylene at different ratios was determined using a bomb calorimeter.

Five different methods were used to calculate the values of thermodynamic factors such as change in enthalpy (ΔH), change in Gibbs free energy (ΔG), and change in Entropy (ΔS) through the following equations [13].

$$\Delta H = E_a - RT \qquad [3]$$

$$\Delta G = E_a + RTln\left(\frac{K_BT}{hA}\right) \qquad [4]$$
$$\Delta S = \left(\frac{\Delta H - \Delta G}{T}\right) \qquad [5]$$

Here, K_B is Boltzmann constant (1.381 x 10^{-23} JK^{-1}) and h is Planck's constant (6.626 x 10^{-34} J-s).

3.2 Thermo-gravimetric analysis

A thermo gravimetric analyzer (TGA 4000, PerkinElmer) was employed to conduct pyrolysis experiments. For each run, Al_2O_3 crucibles were used, and non-isothermal conditions were considered throughout the experiments. The sample was heated from room temperature to a set point of 600 °C. The selected sample was pyrolyzed at heating rates of 10, 20, 30, and 40°C min^{-1} with a nitrogen gas flow rate of 20 ml min^{-1}.

3.3 Kinetic Analysis

Upon using a different approach, kinetic analysis of the thermal decomposition of biomass waste was conducted. The reaction rate $\frac{d\alpha}{dt}$ of the pyrolysis of biomass (RH) and plastic samples (LDPE and PET) can be expressed as follows (Keattch, 1995).

$$\frac{d\alpha}{dt} = K(T) \times F(\alpha) \qquad [6]$$

$$\alpha = \frac{W_i - W_t}{W_i - W_f} \qquad [7]$$

where k is the reaction rate constant (K^{-1}), t is the time (min), α is the reaction conversion, and A is a pre-exponential factor (s^{-1}). R is the universal gas constant (8.314 J mol^{-1}.K^{-1}), and E_a is the activation energy (kJ mol^{-1}). T indicates the temperature in Kelvin; W_i is the sample's initial weight utilized in the experiment.

For non-isothermal pyrolysis, the heating rate (β) can be defined as $\beta = \frac{dT}{dt}$, and the equation is simplified as follows:

$$\beta\frac{d\alpha}{dT} = Aexp\left(-\frac{Ea}{RT}\right) \times F(\alpha) \qquad [8]$$

Accurate determination of kinetic parameters is required for creating a highly effective kinetic model that can explain the pyrolysis procedure. Utilizing TGA data at various heating rates, the activation energy can be determined through iso-conversional (model-free) models like the KAS Equation (9), FWO Equation (10), Starink Equation (11), Freidman Equation (12), and Tang Equation (13). These five models were included in this study due to their widespread popularity.

3.3.1 Iso conversional methods

The iso-conversional approaches function based on the idea that the rate constant (k) is only dependent

on temperature for a reaction and that the degree of conversion is constant. Methods for iso-conversion might be either differential or integral (Acquah et al., 2017). In this research, five iso-conversional techniques, including the Friedman, Tang, Starink, FWO, and KAS approaches, are used to calculate the activation energy. All these methods have been discussed below

3.3.2 Kissinger Akahira Sunose model

$$\ln\left(\frac{\beta}{T^2}\right) = \ln\left(\frac{AE_a}{R_g(\alpha)}\right) - \frac{E_a}{RT} \qquad \textbf{[9]}$$

The value of kinetic parameters for each conversion is represented by the slope of the figure $\ln \beta/T^2$ vs. 1/T. (Akahira & Sunose, 1971).

3.3.3 Flynn Wall Ozawa model

$$\log(\beta) = \log\left(\frac{AE_a}{R_g(\alpha)}\right) - 2.315 - 0.457\frac{E_a}{RT} \qquad \textbf{[10]}$$

The value of kinetic parameter for each conversion is represented by the slope of the linear plot between log (β) and 1/T (Ozawa, 1965).

3.3.4 Starink model

$$\ln\left(\frac{\beta}{T^{1.92}}\right) = \text{constant} - 1.0008\left(\frac{E_a}{RT}\right) \qquad [11]$$

The value of kinetic parameters at each conversion is given by the slope of the graph between $\ln \beta /T^{1.92}$ and 1/T (Kumar et al., 2019).

3.3.5 Friedman method

$$\ln\left(\frac{dx}{dt}\right) = \ln f(x) + \ln A - \frac{E_a}{RT} \qquad [12]$$

The Friedman equation is represented as follows;
The values of the kinetic parameters can be calculated using this equation. A straight line carrying the activation energy is produced by plotting the ln(dx/dt) and 1/T curves (Cai, 2018).

3.3.6 Tang model

$$\ln\left(\frac{\beta}{T^{1.894661}}\right) = C_1 - 1.001450\frac{E_a}{RT} \qquad [13]$$

The value of kinetic parameters at each conversion is given by the slope of the graph between $\ln(\frac{\beta}{T^{1.894661}})$ (and 1/T (Singh et al., 2016).

3.3.7 Comprehensive pyrolysis index

The following comprehensive pyrolysis index (CPI) was used to quantify pyrolysis performance:

$$\text{CPI} = \frac{-(R_a \times R_m) \times M_f}{T_i \times T_p \times \Delta T_{1/2}} \qquad [14]$$

The following parameters can be used to assess the performance of biomass and plastic waste pyrolysis (Zhang et al., 2019).
T_i –initial devolatilization time,
T_p- DTG maximum peak time,
$\Delta T_{1/2}$ - half-peak width range
M_f – final weight loss
R_a - average decomposition rate,
R_m- maximum decomposition rate

CPI- comprehensive pyrolysis index

4. RESULTS AND DISCUSSION

4.1. Physico-chemical characterization

The proximate and elemental compositions of RH, LDPE, and PET are summarized in Table 1. The current samples consist of a significant amount of moisture content in RH (6.75%), 0.02% in PET, and 0.6% in LDPE. In general, biomasses with

lower moisture content (less than 10%) are favored for the pyrolysis process. The results indicated that RH represented low volatile matter (61.8%), but PET and LDPE represented high amounts of volatile matter (87.5% and 98 wt.%) because of high polymeric contents. High organic contents favor the higher heating value and good combustible properties as solid fuel. It is well-identified that high volatile matter content is favorable for thermal decomposition through pyrolysis because they are highly reactive, easily devolatize, and produce substantial amount of bio-oil. RH consists of high ash content (16.8 wt.%), but PET and LDPE presented lesser amounts of ash content (1.8 and 0.1 wt.%). Carbon and hydrogen content were determined through elemental analysis in RH, PET, and LDPE, resulting in 35.84 wt.% and 6.14 wt.%, 63.02 wt.% and 7.92 wt.%, 71.71 wt.% and 15.26 wt.% respectively. PET and LDPE were found to be suitable sources for the pyrolysis process due to their high bio-oil yield and high heating value. The higher heating values observed in PET and LDPE were 18.05 and 21.2 MJ Kg^{-1}. TGA analysis has been depicted below in Fig.1 ,2 and 3 for RH, PET, and LDPE respectively.

Table 1- Physico-chemical Properties of RH, LDPE and PET.

Compositions(weight %)	RH	PET	LDPE
Moisture	6.75	0.02	0.6
Volatile matter	61.8	87.5	98
Ash content	16.8	1.8	0.1
Fixed carbon	14.65	10.68	1.3
Carbon	35.84	63.02	71.71
Hydrogen	6.14	7.92	15.26
Oxygen	57.5	26.21	12.03
Nitrogen	0.44	0.09	0.09
Sulfur	0.1	0	0.92
H/C	2.06	1.51	2.55
O/C	1.20	0.31	0.13
HHV(MJ/kg)	14.81	18.05	21.2

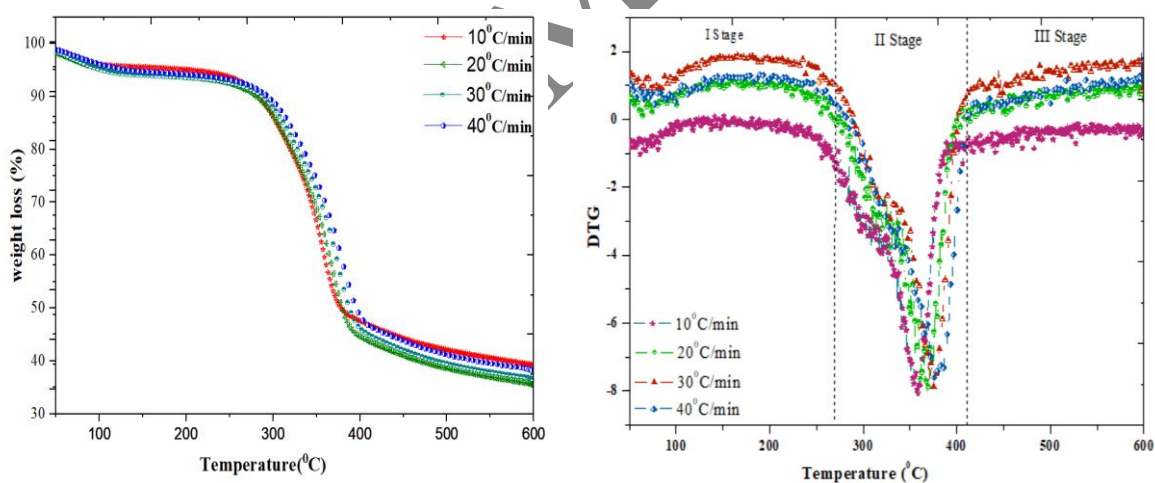**Oxygen and fixed carbon=** calculated by the difference

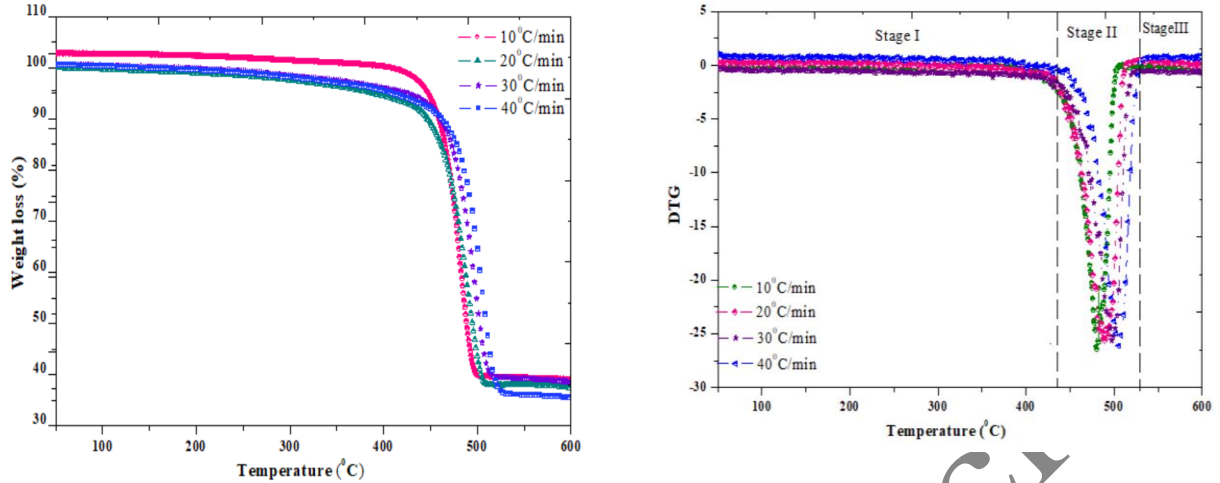Figure 1. TGA and DTG graph of Rice husk at 10, 20, 30 and 40℃/min.

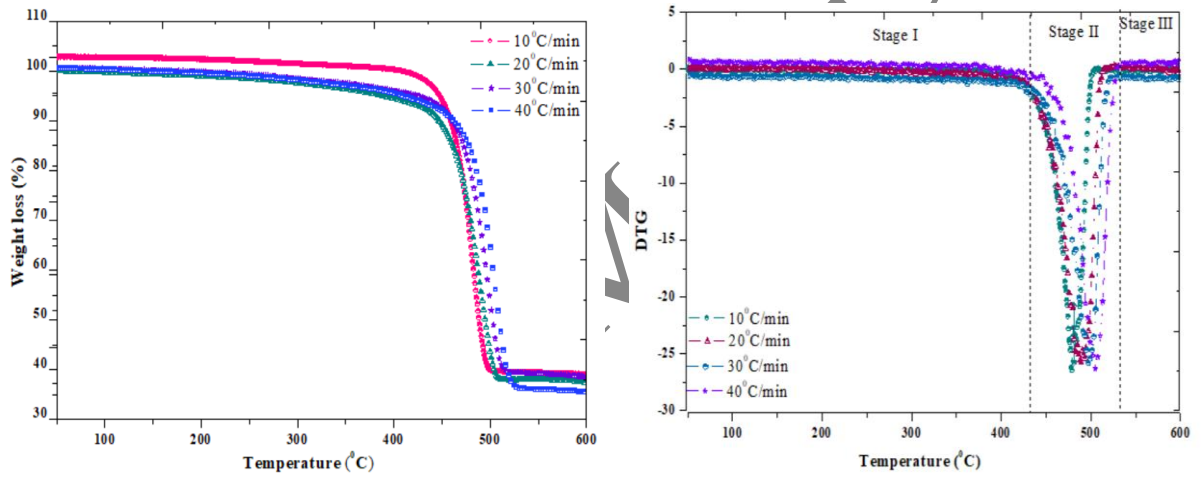Figure 2. TGA and DTG graph of PET at 10, 20, 30 and 40°C/mi

Figure 3. TGA and DTG of LDPE at 10, 20, 30 and 40°C/min.

4.2 Thermal Analysis by TGA and DTG

The degradation process of all three samples in the provided data of RH, LDPE, and PET was examined. However, the initial weight of all samples was only reduced by 0.2% to 5.40% at this stage. However, the initial weight of all samples was only reduced by 0.2% to 5.40% at this stage. The second phase of the volatile region degradation process occurs at higher temperatures, ranging from 200 to 500°C. During this stage, weight loss falls within the range of 43% to 82%. In the third stage, weight loss at the end of the thermal process is between 1% and 10%, observed at temperatures ranging from 500 to 600°C. The thermal characterization is presented in Tables 2, 3, and 4 for RH, LDPE, and PET.

Table 2 Thermal stages of rice husk (RH) in TGA analysis.

β (°C min⁻¹)	First level			Second level			Third level		
	Start	End	Weight Loss (%)	Start	End	Weight Loss (%)	Start	End	Weight Loss (%)
10	30.2	91.2	4	243.7	383.3	48	402	793	14
20	31.8	92.1	5.5	248	385	45	393	604	10
30	30.15	99	5	266	397	44	401	592	9.4
40	30.19	105	3.7	273	402	43	415	600	8

Start refers to the temperature at the start of the stated decomposition process. End refers to the temperature at the end of the stated decomposition stage

Table 3 Thermal stages of low-density polyethylene (LDPE) in TGA analysis

β (°C min⁻¹)	First level			Second level			Third level		
	Start	End	Weight Loss (%)	Start	End	Weight Loss (%)	Start	End	Weight Loss (%)
10	30.8	100	0.2	412	493	82.4	510	796	2.3
20	31.7	82.8	0.6	437	503	53	513	605	1.3
30	31.7	108	1	439	515	54	521	600	1.1
40	31.7	130	1.2	431	522	65	529	601	1

Start refers to the temperature at the start of the stated decomposition process.
End refers to the temperature at the end of the stated decomposition stage

Table 4 Thermal stages of polyethylene terephthalate (PET) in TGA analysis.

β (°C min⁻¹)	First level			Second level			Third level		
	Start	End	Weight Loss (%)	Start	End	Weight Loss (%)	Start	End	Weight Loss (%)
10	30.1	97	1	390	467	80.2	491	798	3.5
20	30.2	91.3	0.2	438	506	63	513	597	1.5
30	30.4	99	0.4	414	486	78.1	492	606	3
40	30.12	97	0.3	418	493	81.8	507	599	2.6

Start refers to the temperature at the start of the stated decomposition process. End refers to the
temperature at the end of the stated decomposition stage

4.3 Kinetic Analysis

Kinetics analysis for the determination of activation energy has been depicted below in Fig. 4, 5, and 6. Iso-conversional methods were used to conduct a kinetic investigation of the thermal behavior of RH, LDPE, and PET. The Flynn-Wall-Ozawa, Kissinger-Akahira-Sunose, Friedman, Starink, and Tang iso-conversional models were used to examine the TGA data at different heating rates of 10 to 40 °C min⁻¹. These methods were chosen to investigate the variation in activation energy results caused by different kinetic parameters. The kinetic parameter in the conversion range of 0.2 to 0.8 was calculated using the slopes of the plots in terms of Eqs. 9 to 11 versus 1/T (weight loss). Table 5, 6, and 7 show the activation energy values at each conversion level, as well as the respective average values for all five models. A detailed explanation of Table 5, 6, and 7 and Figures 4, 5, and 6 shows that activation energy values are obtained using both differential and integral-based methods. The differential-based methods applied in this study were the FWO (Flynn-Wall-Ozawa) method and the Friedman method, while the integral-based methods employed were the KAS (Kissinger-Akahira-Sunose) method, the Starink method, and the Tang method.
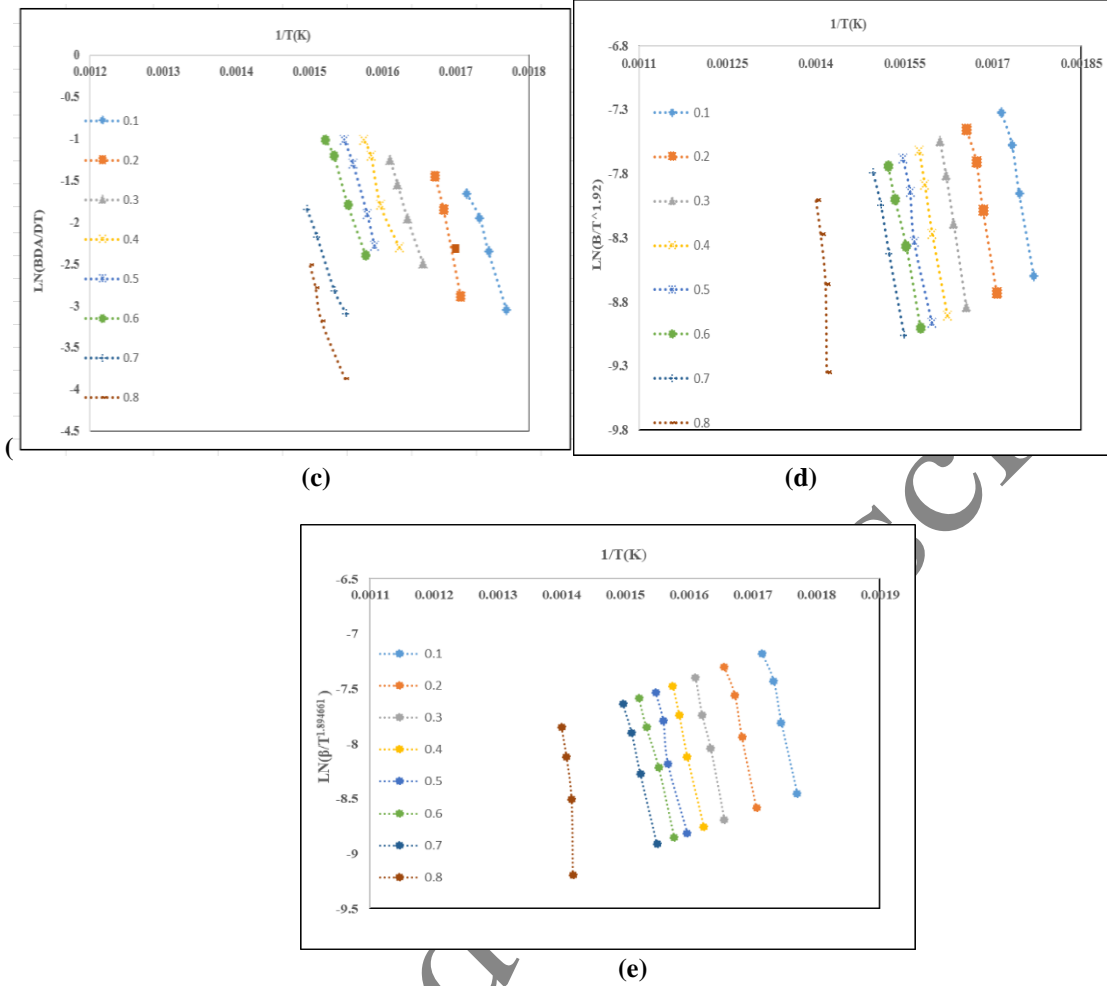

(a)   **(b)**
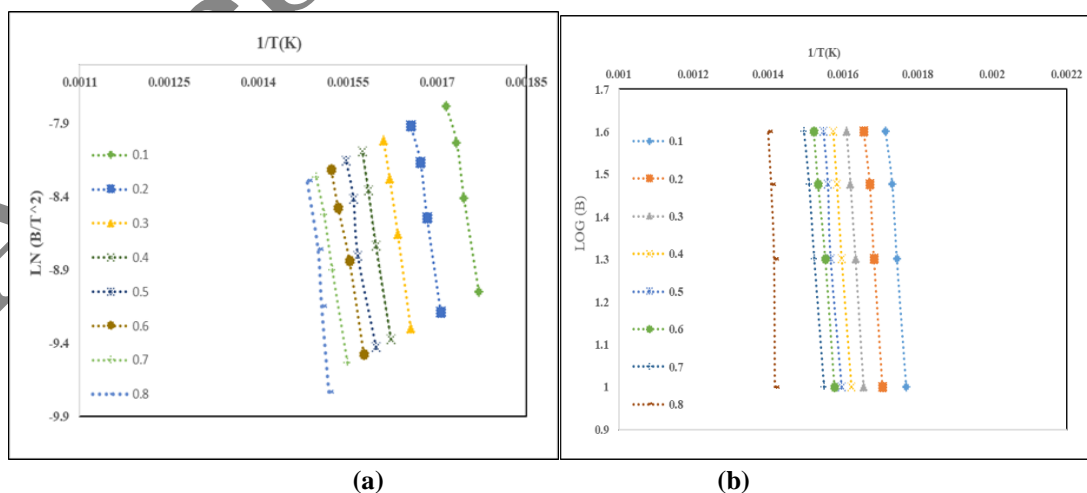
Figure 4. Kinetics graph of RH with 5 different methods (a) KAS Method (b) FWO Method (c) FM Method (d) Starink Method (e) Tang Method

Figure 5. Kinetics graph of LDPE with 5 different methods (a) KAS Method (b) FWO Method (c) FM Method (d) Starink Method (e) Tang Method
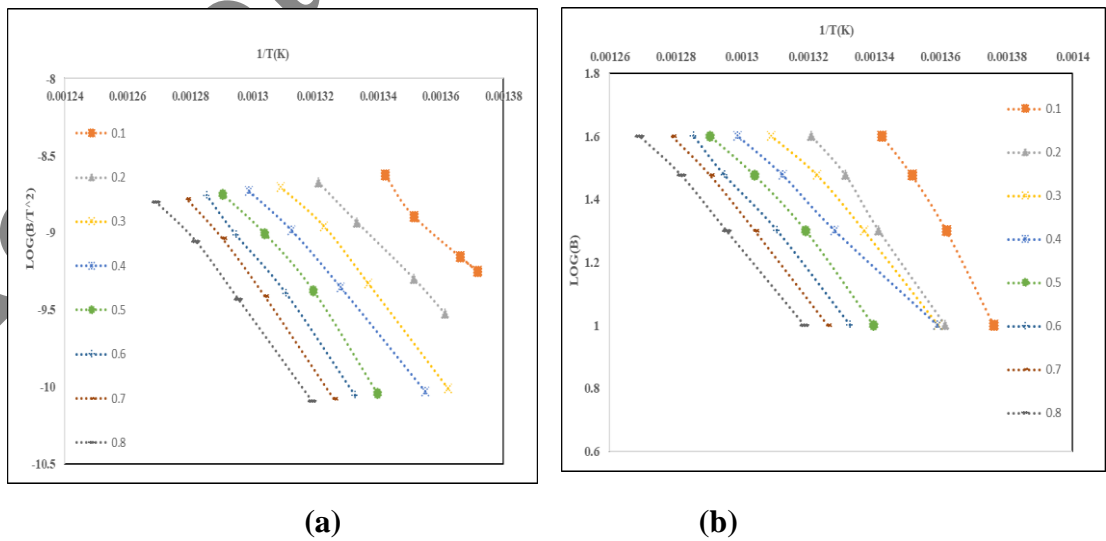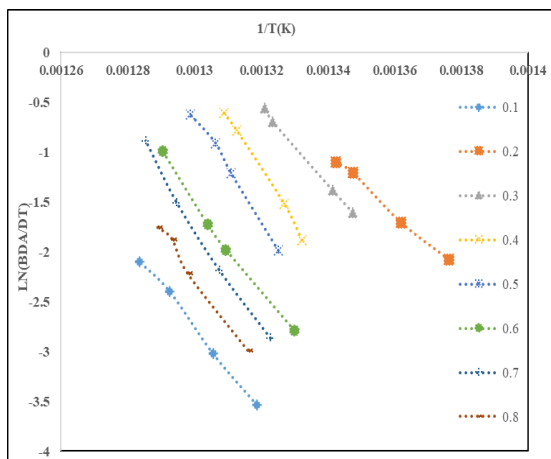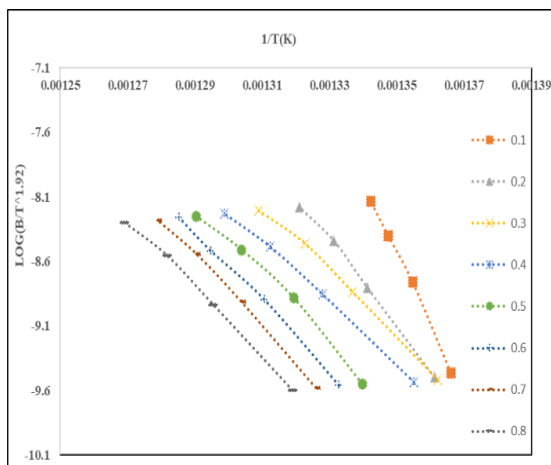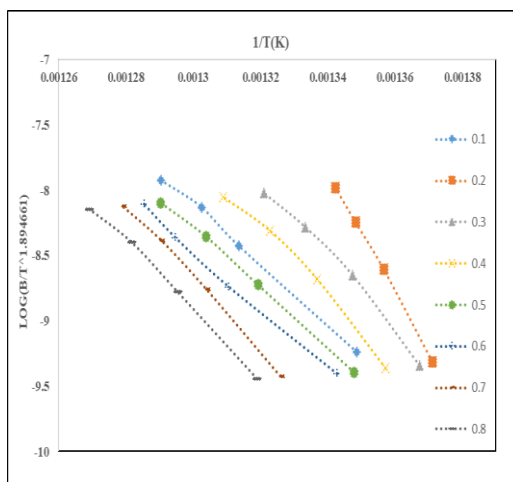
(c)
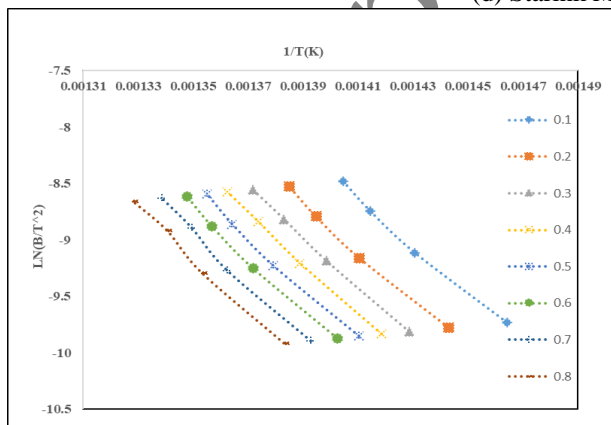

(d)
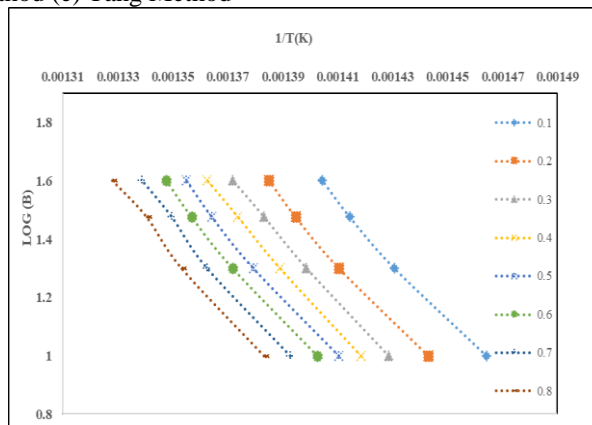

(e)
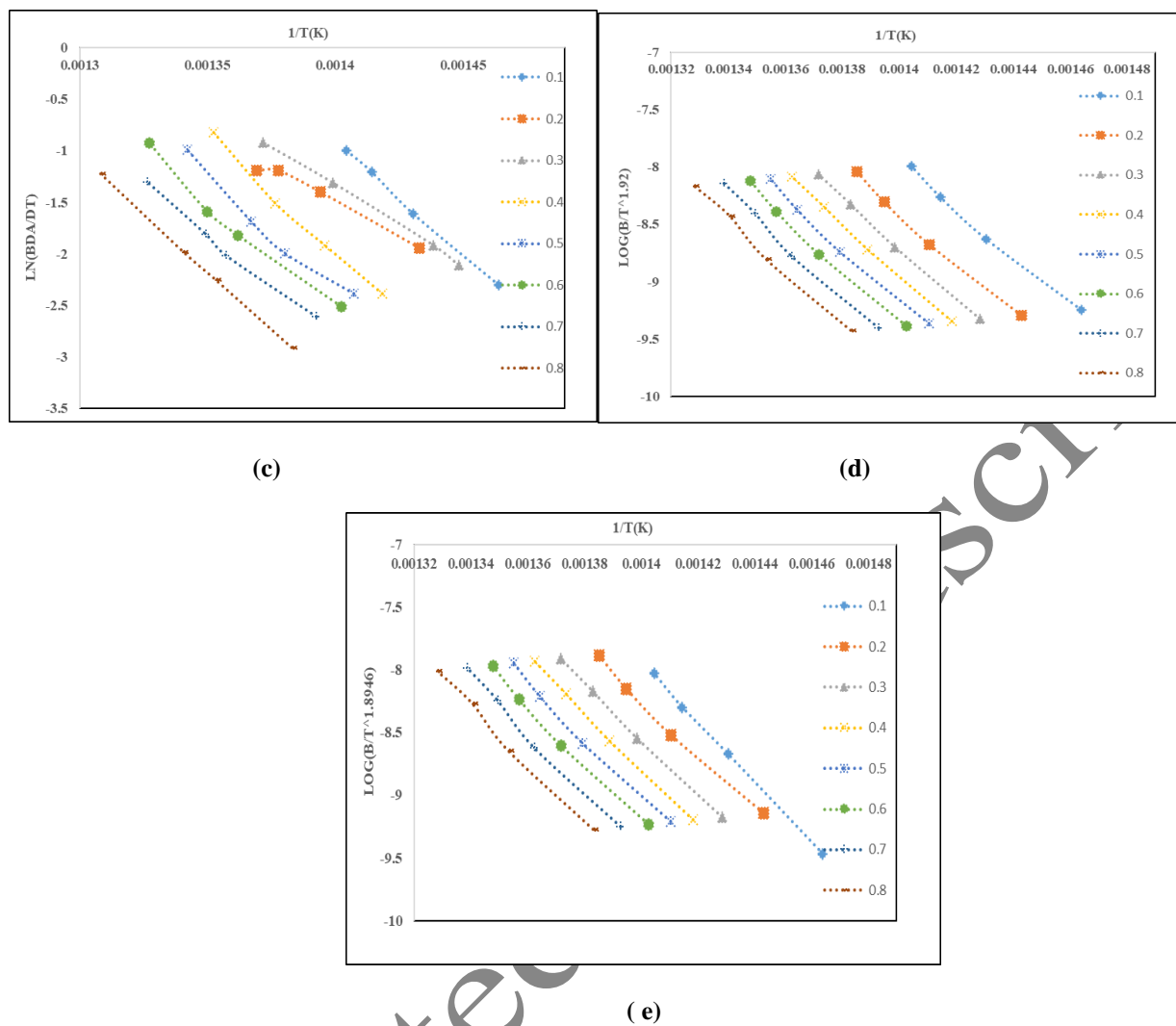
Figure 6. Kinetics graph of PET with 5 different methods (a) KAS Method (b) FWO Method (c) FM Method (d) Starink Method (e) Tang Method

Table 5 Thermal degradation kinetics analysis of RH using iso-conversional methods

| Conversion | Differential method | | | | Integral method | | | | | |
| | FWO | | Friedman | | KAS | | Starink | | Tang | |
	E_a (kJ mol^{-1})	R^2	E_a (kJ mol^{-1})	R^2	E_a (kJ mol^{-1})	R^2	E_a (kJ mol^{-1})	R^2	E_a (Kj mol^{-1})	R^2
0.1	106	0.99	118	0.99	116	0.99	107	0.98	119	0.99
0.2	118	0.99	119	0.99	117	0.99	110	0.99	113	0.99
0.3	113	0.99	122	0.98	121	0.99	112	0.99	118	0.99
0.4	112	0.99	124	0.99	112	0.99	110	0.99	119	0.99
0.5	117	0.99	127	0.99	118	0.99	108	0.98	118	0.99
0.6	111	0.99	130	0.97	117	0.97	107	0.99	119	0.99
0.7	108	0.99	131	0.98	110	0.98	108	0.99	117	0.99
0.8	119	0.99	133	0.98	122	0.98	119	0.96	113	0.99
Average	113	0.98	123	0.98	120	0.98	117	0.97	121	0.99

Table 6 Thermal degradation kinetics analysis of low-density polyethylene using iso-conversional methods.

	Differential method				Integral method					
	FWO		Friedman		KAS		Starink		Tang	
Conversion	E_a (kJ mol^{-1})	R^2	E_a (kJ mol^{-1})	R^2	E_a (kJ mol^{-1})	R^2	E_a (kJ mol^{-1})	R^2	E_a (kJ mol^{-1})	R^2
0.1	102	0.99	103	0.99	106	0.99	104	0.98	109	0.99
0.2	110	0.99	105	0.99	108	0.99	103	0.99	103	0.99
0.3	112	0.99	106	0.98	105	0.99	110	0.99	106	0.99
0.4	110	0.99	104	0.99	104	0.99	105	0.99	107	0.99
0.5	108	0.99	101	0.99	107	0.99	106	0.98	108	0.99
0.6	107	0.99	105	0.97	101	0.97	107	0.99	104	0.99
0.7	114	0.99	110	0.98	108	0.98	108	0.99	109	0.99
0.8	113	0.99	103	0.98	101	0.98	109	0.96	107	0.99
Average	109	0.98	103	0.98	105	0.99	106	0.97	101	0.98

Table 7 Thermal degradation kinetics analysis of polyethylene terephthalate using iso-conversional methods

	Differential method				Integral method					
	FWO		Friedman		KAS		Starink		Tang	
Conversion	E_a (kJ mol^{-1})	R^2	E_a (kJ mol^{-1})	R^2	E_a (kJ mol^{-1})	R^2	E_a (kJ mol^{-1})	R^2	E_a (kJ mol^{-1})	R^2
0.1	115	0.99	108	0.99	119	0.99	119	0.99	117	0.99
0.2	117	0.99	103	0.99	120	0.99	117	0.99	113	0.99
0.3	112	0.99	102	0.99	123	0.99	110	0.99	114	0.99
0.4	111	0.99	101	0.99	116	0.99	112	0.99	117	0.99
0.5	115	0.99	105	0.99	117	0.99	114	0.99	116	0.99
0.6	117	0.99	110	0.97	118	0.97	116	0.99	119	0.99
0.7	102	0.99	109	0.98	110	0.98	118	0.99	119	0.99
0.8	100	0.99	108	0.98	119	0.98	110	0.99	115	0.99
Average	111	0.98	105	0.98	117	0.98	114`	0.99	115	0.98

The average activation energy values for rice husk, low-density polyethylene, and polyethylene terephthalate were determined using the FWO method, resulting in values of 113 kJ mol^{-1}, 109 kJ mol^{-1}, and 111 kJ mol^{-1}, respectively. These results indicate that LDPE and PET are more suitable as feedstock for the pyrolysis process as they have a lower activation energy requirement. In addition, the activation energy values were also calculated using the Friedman method, resulting in 123 kJ mol^{-1}, 103 kJ mol^{-1}, and 105 kJ mol^{-1}, respectively. The KAS method resulted in 120 kJ mol^{-1}, 105 kJ mol^{-1}, and 117 kJ mol^{-1}, respectively; the Starink method resulted in 117 kJ mol^{-1}, 106 kJ mol^{-1}, and 114 kJ mol^{-1}, respectively. ; the Starink method resulted in 117 kJ mol^{-1}, 106 kJ mol^{-1}, and 114 kJ mol^{-1}, respectively. The Tang method reported the activation energy values of 121 kJ mol^{-1}, 101 kJ mol^{-1}, and 115 kJ mol^{-1}, respectively. These results provide a comprehensive understanding of the thermal behavior and kinetic parameters of RH, LDPE, and PET for pyrolysis. Furthermore, it can be inferred that by comparing the results obtained from different methods,

a more accurate and reliable conclusion can be drawn about the suitability of these materials as feedstocks for pyrolysis. These results indicate that LDPE and PET are more suitable as feedstock for the pyrolysis process as they have a lower activation energy requirement. The major pyrolysis process begins when Ea values for conversions in the range of 0.1 to 0.3 increase sharply, while Ea values for conversions in the range of 0.3 to 0.8 indicate that the reaction has reached the charring stage, which results in similarly high Ea values. The best-fitting curves for conversions between 0.2 and 0.8 are also shown in Figs. 4,5, and 6, demonstrating that the response mechanism is the same for all conversions. The dependency of apparent activation energy on temperature and conversion ratio is confirmed by a progressive rise in apparent activation energy values with an increase in conversion ratio (Nawaz & Kumar, 2022).

4.4 Pyrolysis performance index

The Comprehensive Pyrolysis Index (CPI) significantly improved with an increasing heating rate. It was observed that an increased heating rate favors pyrolysis, as shown in Table 8. The entire Volatile Release Index (CPI) for RH, LDPE, and PET at 600 °C in N$_2$ atmospheres ranged from 0.4 to 4.5, 2.02 to 8.5, and 1.6 to 7.5 times that of the reactions in the entire process, respectively. In other words, the high heating rate was more conducive to the pyrolysis of all the samples at 600 °C.R$_a$ (Average Decomposition Rate), R$_m$ (Maximum Decomposition Rate), and CPI values all showed a significant increase, indicating that the high heating rate improves pyrolysis performance. The CPI index is calculated using Equation 14. Further details on the CPI of RH, PET, and LDPE are provided in Table 8.

Table 8 CPI analysis of three different samples at four different heating rates.

Sample	β	T$_i$	T$_p$	R$_a$	R$_m$	ΔT$_{1/2}$	CPI
RH	10	215.2	356.2	-1.12	-8.10	87.3	0.4
	20	272.9	369.4	-2.16	-15.3	81.7	1.5
	30	279.5	376.2	-3.19	-22.3	75.7	3.4
	40	292.6	381.5	-4.29	-28.08	78.9	4.5
PET	10	383.5	440.29	-1.48	-20.5	37.5	1.6
	20	405.5	454.04	-2.91	-41.09	38.2	2.4
	30	412.3	466.17	-4.26	-63.7	37.2	5.5
	40	424.8	469.59	-5.66	-84.7	38.11	7.5
LDPE	10	414.02	480.7	-1.518	-26.32	38.2	2.02
	20	431.5	492.7	-2.120	-27.7	51.8	3.61
	30	439.1	498.01	-3.067	-46.07	48.02	5.1
	40	448.7	505.2	-4.203	-64.9	45.9	8.5

4.5 Thermodynamic Analysis

Rice husk degradation is influenced by varying temperature due to the cellulose, hemicellulose, and lignin contents. Hemicellulose primarily loses weight between 220 and 315 °C, while cellulose primarily loses weight between 315 and 400 ºC. Lignin, on the other hand, proves more challenging to break down since it loses weight throughout a large temperature range (from 160 to 900 ºC) and produces a large amount of solid residue (40 wt%). From the perspective of the energy used during the pyrolysis process (Haiping Yang et al., 2007). The weight loss peaks of the hemicellulose and cellulose decompositions are the first and second absorption peaks of the DTG curve. The differential thermo-gravimetric (DTG) analysis of RH, LDPE, and PET is shown in

Fig. 2-4 as a function of temperature at four different heating speeds of 10, 20, 30, and 40 °C min^{-1}. At lower temperatures, the rate of mass loss is quite modest; nevertheless, it increases during the second stage of the process. Due to the production of char at 500°C, the rate of mass loss is once again modest. The DTG peaks are visible in the RH sample at 356, 369, 376, and 381°C at heating rates of 10, 20, 30, and 40 °C min^{-1} in the second stage of degradation, and LDPE at temperature peaks at 480, 492, 498, and 505 °C, and polyethylene terephthalate at a peak temperature of 440, 454, 466, and 469°C respectively. The location and size of the DTG peak are affected by the heating rate. By examining Fig. 1, 2, 3, an increase in heating rate results in the peak shifting towards a higher temperature because the response time is shorter at higher heating rates, meaning that a higher temperature is needed for deterioration (Chen et al., 2022).For common biomasses such as sawdust, seaweed, almond fruit,and garlic husk, similar observational trends in

TGA and DTG curves have been noted (Olszak-Humienik & Mozejko, 2000; Agnihotri et al., 2022). Peak decomposition temperatures are 307°C,314.54 °C, 320.81 °C, and 330.86 °C for the heating rates of 5°C,10°C, 15°C, and 20°C min⁻¹, respectively. The breakdown reaction of RH, LDPE, and PET is also inferred from the TG and DTG plots to follow a multi-step kinetic reaction mechanism with several inflection points. The slight increase in peak temperatures indicates that increasing the heating rate did not influence the form of DTG profiles or the quantity of mass loss [Vyazovkin et al.2020]. This increase in maximum decomposition temperature with increasing heating **r**ate might be attributable to increased heat transport constraints. A higher heating rate indicates that the quantity of time the biomass is kept at a specific temperature is significantly shorter, resulting in uneven heating throughout the volume of the biomass. As a result, a higher temperature is required to complete the degradation of the same amount of biomass at higher heating rates (Singh et al., 2020)**.** The thermodynamic parameters and their interaction might be utilized to describe distinct phases of biomass breakdown efficiently. Equations 1-3 were used to calculate the thermodynamic parameters obtained for each model-free iso-conversional technique. For several models, the variance of change in enthalpy (ΔH) and change in Gibbs free energy (ΔG) values has been estimated. The change in enthalpy (H) in a chemical reaction represents the energy difference between the reactants and products. It also provides information on whether the reaction is exothermic or endothermic. In this study, there is very little (~ 5 kJ mol⁻¹) energy between activation energy and change in enthalpy,

indicating that the chemical reaction begins quickly. The low difference between activation energy (Ea) and enthalpy (H) facilitates the synthesis of activated complexes and shows that the products are readily produced with minimal additional energy (Vyazovkin et al., 2020). The change in Gibbs free energy (G) change of any system at a specific temperature and pressure is used to determine the maximum amount of work. It's a thermodynamic "state function" that demonstrates how much energy a biomass sample can produce (Kumar et al., 2020).Table 9, given below, illustrates the frequency factor and thermodynamic triplets of the selected samples. It indicates that a change in entropy (S) value means the material has crossed the energy barrier and is approaching equilibrium. The material is less reactive in this state, and product formation takes a long time. A high value of (S), on the other hand, indicates that the material reacts quickly and produces a product in less time (Ruvolo-Filho & Curti, 2006). The tendency for ΔS to take on positive values also corresponds to the tendency for the decomposition process to become more disorderly, primarily as a result of the devolatilization phase, which necessitates a gradual increase in energy input until all volatiles have broken free from the solid. The reaction suffers less resistance because of lower levels of disorderliness, as indicated by the negative ΔS values seen at lower conversions, which are consistent with earlier results (Kumar et al., 2020). The minimum entropy indicates less disorder during the reaction. The results for distinct thermodynamic parameters that were calculated using five different iso-conversional model-free approaches were very similar, supporting the validity of the thermodynamic study and the findings. The pyrolysis reaction may be thoroughly examined using these data and conclusions linking changes in thermodynamic parameters to various phases of the breakdown mechanism. Thermodynamics characterization analyzed by DTG has been depicted below in Table 9, and nomenclature has been given in Table 10.

Table 9 Thermodynamic parameter of all three samples with five different methods.

Methods												
	The conversion used during the analysis from 0.1 to 0.8											
	RICE				**LDPE**				**PET**			
	A	**ΔH**	**ΔG**	**ΔS**	**A**	**ΔH**	**ΔG**	**ΔS**	**A**	**ΔH**	**ΔG**	**ΔS**
KAS	3.7E+15	114	130	-0.062	3.6E+11	100	116	-0.038	2.6E+8	111	126	-0.052
FWO	2.9E+17	107	124	-0.066	1.7E+10	103	119	-0.047	2.8E+10	105	116	-0.049
FRIED-MAN	5.5E+16	118	137	-0.074	1.2E+16	98	117	-0.040	2.7E+11	100	118	-0.055
STARINK	7.6E+15	111	129	-0.070	1.5E+19	101	115	-0.042	2.5E+10	98	114	-0.065
TANG	6.4E+15	115	135	-0.078	2.4E+13	95	105	-0.050	2.1E+9	109	126	-0.057

*ΔH-kJ mol⁻¹; ΔG-kJ mol⁻¹; ΔS-kJmol⁻¹ K⁻¹.

5. CONCLUSIONS
The present study provides valuable insights into the thermal decomposition properties of different wastes at various heating rates by utilizing both the differential and integral methods. The kinetic parameters, including activation energy and pre-exponential factor, were successfully determined. The average activation energy values for RH, LDPE, and PET were determined using the five different methods, resulting in the value range of 113-123 kJmol⁻¹, 101-109 kJ mol⁻¹, and 105-117 kJ mol⁻¹, respectively. These results indicate that LDPE and PET are more suitable as feedstock for the pyrolysis process as they have a lower activation energy requirement. The

average values of thermodynamic triplets such as ΔH, ΔG, and ΔS are recorded in the range of 99.4- 113 kJ mol^{-1}, 105-131 kJ mol^{-1}, and -0.043 to -0.07, respectively. This indicates that the reaction is endothermic and non-spontaneous in nature.

Additionally, the parameters of thermodynamic parameters and pyrolysis performance index of all three sampleswere thoroughly analyzed by kinetics. The kinetic analysis of all materials used in this work is significant and helpful for the design of a contemporary pyrolysis reactor.

6. Scope of study and future recommendation

The present study makes significant contributions to the understanding of waste selection for thermochemical conversion procedures, such as gasification, pyrolysis, and combustion. . By assessing the temperature range and heating rates, Thermogravimetric Analysis (TGA) and Derivative Thermogravimetry (DTG) can help determine the optimal conditions for endothermic or exothermic reactions during pyrolysis and gasification. This method reduces expenses for further processing and saves time. Furthermore, the study is enhanced by the inclusion of Comprehensive Pyrolysis Index (CPI) data, providing details on higher heating values and thermal stability. These results facilitate well-informed decision-making for upcoming energy production projects. While the study does not explicitly discuss the use of software tools to forecast activation energy or thermal stability (entropy or enthalpy), it emphasizes the importance of these concepts for a thorough investigation.

7. ACKNOWLEDGEMENT

NOMENCLATURE

kJmol-1	KiloJoule mole-1
FWO	Flynn-Wall-Ozawa
KAS	Kissinger-Akahira-Sunose
TG	Thermogravemetric
DTG	Derivative Thermogravemetric
K	Kinetic rate constant
C/min	Degree centigrade per minute
PET	Polyethylene Terephthalate
LDPE	Low-Density Polyethylene
RH	Rice husk
CHNS	Carbon hydrogen nitrogen sulphur
Δ_G	Gibbs free energy
Δ_S	Entropy
Ea	activation energy
Δ_H	Enthalpy
HHV	Higher-heating vvalue
WC	Water content
VM	volatile matter
FC	Fixed carbon
AC	ash content
CPI	Pyrolysis performance index

REFERENCES

1. Acquah, G. E., Via, B. K., Fasina, O.O., Adhikari S., Billor S., Eckhardt, L. G. (2017)."Chemometric Modeling of Thermogravimetric Data for the Compositional Analysis of Forest Biomass". PLoS ONE, Vol.12, No. 3 (2017), e0172999. (https://dx.doi.org/10.1371/journal.pone.0172999).

2. Agnihotri, N., Gupta, G. K., Mondal, M. K. (2022). "Thermo-Kinetic Analysis, Thermodynamic Parameters, and Comprehensive Pyrolysis Index of Melia Azedarach Sawdust as a Genesis of Bioenergy". Biomass Conversion and Biorefinery, (2022), 1-18. (https://doi.org/10.1007/s13399-022-02524-y).

3. Akahira, T., Sunose, T. (1971). "Method of Determining Activation Deterioration Constant of Electrical Insulating Materials". Research Report, Chiba Institute of Technology, 16, 22–23. (https://doi.org/10.1016/j.softx.2019.100359)

4. Cai, J. (2018). "Processing Thermogravimetric Analysis Data for Isoconversional Kinetic Analysis of Lignocellulosic Biomass Pyrolysis: Case Study of Corn Stalk". Renewable and Sustainable Energy Reviews, Vol. 82, 2705-2715. (http://dx.doi.org/10.1016/j.rser.2017.09.113)

5. Chen, W., Escalante, J., Chen, W., Tabatabaei, M., Tuan, A. (2022). "Pyrolysis of Lignocellulosic, Algal, Plastic, and Other Biomass Wastes for Biofuel Production and Circular Bioeconomy". Renewable and Sustainable Energy Reviews, 169 (2022) 112914. (https://doi.org/10.1016/j.rser.2022.112914)

6. Keattch, C. (1995). "Studies in the History and Development of Thermo-Gravimetry". Journal of Thermal Analysis, Vol. 44, No. 5 (1995), 1211-1218. (https://doi.org/10.1007/BF01905580).

7. Kumar, M., Sabharwal, S., Mishra, P. K., Upadhyay, S. N. (2019). "Thermal Degradation Kinetics of Sugarcane Leaves (Saccharum Officinarum L) Using Thermo-Gravimetric and Differential Scanning Calorimetric Studies". Bioresource Technology, Vol. 279 (2019) 262-270. (10.1016/j.biortech.2019.01.137.

8. Kumar, M., Upadhyay, S. N., & Mishra, P. K. (2020). "Effect of Montmorillonite Clay on Pyrolysis of Paper Mill Waste". Bioresource Technology, Vol. 307(2020),123161. (https://doi.org/10.1016/j.biortech.2020.123161).

9. Nawaz, A., Kumar, P. (2022). "Pyrolysis Behavior of Low-Value Biomass (Sesbania Bispinosa) to Elucidate Its Bioenergy Potential: Kinetic, Thermodynamic, and Prediction Modeling Using Artificial Neural Network". Renewable Energy, Vol. 200 (2022) 257–270 (https://doi.org/10.1016/j.renene.2022.09.110).

10. NPTEL. report . "Thermogravimetric Analysis", 2016, Retrieved from (https://nptel.ac.in/courses/115103030/21).

11. Olszak-Humienik, M., Mozejko, J. (2000). "Thermodynamic Functions of Activated Complexes Created in Thermal Decomposition Processes of Sulphates". Thermochimica Acta, Vol. 344, No.1-2 (2000), 73–77, (https://doi.org/10.1016/S0040-6031(99)00329-9).

12. Ozawa, T. (1965). "A New Method of Analyzing Thermogravimetric Data". Bulletin of the Chemical Society of Japan, 38 (1965) 1881–1886. (https://doi.org/10.1246/bcsj.38.1881).

13. Rahman, M. (2022). "Test and performance optimization of nozzle inclination angle and swirl combustor in a low-tar biomass gasifier: a biomass power generation system perspective", Carbon Resources Conversion. Vol. 5, No. 2 (2022), 139-149. (https://doi.org/10.1016/j.crcon.2022.01.002).

14. Rahman, M., Henriksen, U.B., Ahrenfeldt, J., Arnavat, M.P. (2020). "Design, construction and operation of a low-tar biomass (LTB) gasifier for power applications", Energy, 204(2020), 117944. (https://doi.org/10.1016/j.energy.2020.117944).

15. Ruvolo-Filho, A., Curti, P. S. (2006). "Chemical Kinetic Model and Thermodynamic Compensation Effect of Alkaline Hydrolysis of Waste (Polyethylene Terephthalate) in Non-Aqueous Ethylene Glycol Solution", Industrial & Engineering Chemistry Research, Vol.45(2006), 7985–7996. (https://doi.org/10.1021/ie060528y).

16. Singh, R. K., Patil, T., Sawarkar, A. N. (2020). "Pyrolysis of Garlic Husk Biomass: Physicochemical Characterization Thermodynamic and Kinetic Analyses". Bioresource Technology Reports, 12 (2020) 100558. (https://doi.org/10.1016/j.biteb.2020.100558).

17. Singh, R. K., Ruj, B., Evrendilek, F. (2016). "Time and Temperature Dependent Fuel Gas Generation from Pyrolysis of Real World Municipal Plastic Waste", Fuel, 174 (2016) 164–171. (https://doi.org/10.1016/j.fuel.2016.01.049).

18. Vyazovkin, S., Burnham, A. K., Favergeon, L., Koga, N., Moukhina, E., P´erez-Maqueda, L. A., Sbirrazzuoli, N. (2020). ICTAC "Kinetics Committee Recommendations for Analysis of Multi-StepKinetics". Thermochimica Acta, Vol.689, 178597. (https://doi.org/10.1016/j.tca.2020.178597).

19. Vyazovkin, S., Wight, C.A. (1998). "Isothermal and non-isothermal kinetics of thermally stimulated reactions of solids", International Reviews in Physical Chemistry, Vol. 17, No.3 (1998) 407-433. (https://doi.org/10.1080/014423598230108).

20. Yang H., Yan R., Chen H., Lee D.H., Zheng C. (2007). "Characteristics of hemicellulose, cellulose, and lignin pyrolysis" Vol. 86, No. 12–13(2007), 1781-1788. (https://doi.org/10.1016/j.fuel.2006.12.013).

21. Zhang, J., Liu, J., Evrendilek, F., Zhang, X., Buyukada, M. (2019). "TG-FTIR and Py-GC/MS Analyses of Pyrolysis Behaviors and Products of Cattle Manure in CO2 and N2 Atmospheres: Kinetic, Thermodynamic, and Machine-Learning Models". Energy Conversion and Management, 195 (2019) 346–359. (https://doi.org/10.1016/j.enconman.2019.05.019).

22. Zhang, L., Xu, C., Champagne, P. (2010). "Overview of Recent Advances in Thermo-Chemical Conversion of Biomass". Energy Conversion and Management, Vol. 51, No.5, (2010), 969-982. (https://doi.org/10.1016/J.ENCONMAN.2009.11.038).